THE JOURNAL OF BIOLOGICAL CHEMISTRY VOL. 287, NO. 25, pp. 21416–21428, June 15, 2012

Protein Kinase C (PKC) Activity Regulates Functional Effects of $K_v\beta1.3$ Subunit on $K_V1.5$ Channels

IDENTIFICATION OF A CARDIAC $K_v1.5$ CHANNELOSOME[*S]*

Received for publication, December 2, 2011, and in revised form, April 13, 2012 Published, JBC Papers in Press, April 30, 2012, DOI 10.1074/jbc.M111.328278

Miren David[‡1,2], Álvaro Macías[‡1,3], Cristina Moreno[‡4], Ángela Prieto[‡4], Ramón Martínez-Mármol[§], Rubén Vicente[¶], Teresa González[‡5], Antonio Felipe[§], Michael M. Tamkun[‖], and Carmen Valenzuela[‡6]

From the [‡]Instituto de Investigaciones Biomédicas, Madrid Consejo Superior de Investigaciones Científicas-Universidad Autónoma de Madrid, C/Arturo Duperier 4, 28029 Madrid, Spain, the [§]Molecular Physiology Laboratory, Departamento de Bioquímica i Biología Molecular, Institut de Biomedicina (IBUB). Universitat de Barcelona, 08028 Barcelona, Spain, the [¶]Laboratory of Molecular Physiology and Channelopathies, Department of Experimental and Health Sciences, Universitat Pompeu Fabra, Edifici PRBB, C/Dr. Aiguader 88, 08003 Barcelona, Spain, and the [‖]Program in Molecular, Cellular, and Developmental Neuroscience, Department of Biomedical Sciences and Department of Biochemistry and Molecular Biology, Colorado State University, Fort Collins, Colorado 80523

Background: $K_v\beta1.3$ fast inactivation conferred onto $K_v1.5$ is PKC-dependent.
Results: PKC inhibition shifts $K_v\beta1.3$-induced inactivation curve without altering $K_v1.5$-$K_v\beta1.3$ interaction. A $K_v1.5$ channelosome is characterized.
Conclusion: $K_v1.5$ channelosome is composed of several PKC isoforms (βI, βII, and θ), $K_v\beta1.3$ and RACK1 in HEK293 and in rat ventricular cells.
Significance: This is the first evidence of a cardiac Kv1.5-$K_v\beta1.3$-RACK1-PKC macromolecular complex.

$K_v1.5$ channels are the primary channels contributing to the ultrarapid outward potassium current (I_{Kur}). The regulatory $K_v\beta1.3$ subunit converts $K_v1.5$ channels from delayed rectifiers with a modest degree of slow inactivation to channels with both fast and slow inactivation components. Previous studies have shown that inhibition of PKC with calphostin C abolishes the fast inactivation induced by $K_v\beta1.3$. In this study, we investigated the mechanisms underlying this phenomenon using electrophysiological, biochemical, and confocal microscopy approaches. To achieve this, we used HEK293 cells (which lack $K_v\beta$ subunits) transiently cotransfected with $K_v1.5$+$K_v\beta1.3$ and also rat ventricular and atrial tissue to study native α-β subunit interactions. Immunocytochemistry assays demonstrated that these channel subunits colocalize in control conditions and after calphostin C treatment. Moreover, coimmunoprecipitation studies showed that $K_v1.5$ and $K_v\beta1.3$ remain associated after PKC inhibition. After knocking down all PKC isoforms by siRNA or inhibiting PKC with calphostin C, $K_v\beta1.3$-induced fast inactivation at +60 mV was abolished. However, depolarization to +100 mV revealed $K_v\beta1.3$-induced inactivation, indicating that PKC inhibition causes a dramatic positive shift of the inactivation curve. Our results demonstrate that calphostin C-mediated abolishment of fast inactivation is not due to the dissociation of $K_v1.5$ and $K_v\beta1.3$. Finally, immunoprecipitation and immunocytochemistry experiments revealed an association between $K_v1.5$, $K_v\beta1.3$, the receptor for activated C kinase (RACK1), PKCβI, PKCβII, and PKCθ in HEK293 cells. A very similar $K_v1.5$ channelosome was found in rat ventricular tissue but not in atrial tissue.

The outward potassium current I_{Kur},[7] the main current responsible for human atrial repolarization, is generated following the activation of $K_v1.5$ channels. The slow and partial inactivation and the voltage dependence of these channels underlie their key role in the regulation of the atrial action potential duration (1, 2). This slow inactivation is modified by the assembly of $K_v1.5$ subunits with β subunits ($K_v\beta1.2$, $K_v\beta1.3$, and $K_v\beta2.1$) present in the human myocardium (3, 4). The $K_v\beta1.3$ subunit provides a number of functions, including a fast, partial inactivation component, a greater degree of slow inactivation, a shift of the activation curve toward more negative potentials, a 7-fold decrease in the sensitivity of the channel to the block induced by antiarrhythmic drugs and local anesthetics, and a decrease in the degree of stereoselective blockage (5–7).

I_{Kur} is highly susceptible to adrenergic regulation, which is differentially modulated by α- and β-stimulation (8) via protein kinases C (PKC) and A (PKA), respectively (9–11). This phenomenon is very important because the expression levels of α-

* This work was supported by Ministerio de Ciencia e Innovación (MICINN) Grants SAF2010-14916, Ministerio de Educación y Ciencia-PR2003-0056, and Red Cooperativa de Enfermedades Cardiovasculares RECAVA FIS RD06/0014/0006 (to C. V.) and BFU2011-23268 and CSD2008-00005 (to A. F.).
[S] This article contains supplemental Fig. S1 and Table S1.
[1] Both authors contributed equally to this work.
[2] Recipient of an RECAVA grant.
[3] Recipient of a JAE predoctoral grant.
[4] Recipients of an FPI grant.
[5] Recipient of a JAE doctoral grant.
[6] Recipient of Grant MEC-PR2003-0056. To whom correspondence should be addressed: Instituto de Investigaciones Biomédicas 'Alberto Sols' (CSIC-UAM), Laboratory 1.13, C/Arturo Duperier 4, 28029 Madrid, Spain. Tel.: 34-91-585-4493; Fax.: 34-91-585-4401; E-mail: cvalenzuela@iib.uam.es.

[7] The abbreviations used are: I_{Kur}, ultrarapid delayed outward rectifying current; PLC, phospholipase C; RACK1, receptor for activated protein kinase C; DAG, diacylglycerol; OAG, 1-oleoyl-2-acetyl-*sn*-glycerol; PIP, phosphoinositide; PIP_2, phosphatidylinositol 4,5-bisphosphate; IP_3, inositol 1,4,5-trisphosphate; IP_3R, IP_3 receptor.

and β-adrenergic receptors are altered in several cardiac pathologies as well as the release of catecholamines (12, 13). In fact, cardiac hypertrophy is associated with an up-regulation of different PKC isoforms (14–17). Similarly, δ-calmodulin kinase II (δ-CaMKII) expression increases during atrial fibrillation (18). Furthermore, one of the most effective treatments for atrial fibrillation is the oral administration of β-blockers (19), which induce a pharmacological remodeling that is capable of reversing the electrical dysfunction typically observed during atrial fibrillation (20, 21). PKC and PKA activities are also required for the Kv1.5 modulation by the auxiliary subunits $K_v\beta1.2$ and $K_v\beta1.3$ (9, 10, 22). Indeed, PKC inhibition by calphostin C reverses the $K_v\beta1.3$-dependent electrophysiological effects (9). Calphostin C, a potent and selective inhibitor of multiple protein kinase C (PKC) isoforms, acts via interaction with the regulatory diacylglycerol (DAG) binding site (23).

PKCs comprise a cluster of at least 11 different isoforms that include three subfamilies according to their sensitivities to second messengers such as Ca^{2+} and DAG. Classical isoforms (PKCα, -βI, -βII, and -γ) are activated by Ca^{2+} and DAG, whereas novel isoforms (PKCδ, -ϵ, -η, and θ) are sensitive to DAG but insensitive to Ca^{2+}. Finally, atypical isoforms (PKCζ and λ/ι) do not require Ca^{2+} or DAG for their activation, whereas they are dependent on ceramide, arachidonic acid, and other lipids (24–26). Upon activation, most PKC isoforms undergo subcellular relocation depending on the cell type (27). This specific compartmentation is further fine-tuned by interactions with specific PKC adaptor proteins named receptor for activated C kinase (RACK) (28).

PKC isoforms translocate to different subcellular sites after their activation by specific second messengers, eliciting unique cellular effects (29, 30) that are dependent on the substrate to be phosphorylated (26, 31). The interaction of PKCs with several substrates is believed to occur through a family of proteins that are collectively named RACKs (32). These adaptor proteins do not have any intrinsic functional effects. However, they are able to translocate bound proteins to different subcellular locations through their protein-protein interaction domains (WD40) (33). Thus, they are capable of binding several enzymes concomitantly to form an enzymatic complex that is localized close to the substrate of the enzyme. This process allows them to regulate different cellular responses (32). RACK1 is one of the adaptor proteins that has been identified as an anchoring protein for PKC. Additionally, several ion channels ($K_{Ca}1.1$, $Ca_v1.2$, $K_{ir}3.1$, TRPC3, and NMDA receptor) have been reported to be modulated by PKC via this scaffold protein (34–39). The binding of RACK1 to PKCβII enhances the enzymatic activity of the latter by 4–6-fold (34, 40).

In the present study, we analyzed the effects of PKC inhibition on the $K_v1.5$+$K_v\beta1.3$ interaction. None of the isoform-selective PKC inhibitors removed the $K_v\beta1.3$-mediated fast inactivation. By silencing all of the PKC isoforms with siRNA or inhibiting PKCs with calphostin C, fast inactivation was abolished at membrane potentials up to +60 mV. However, at membrane potentials more positive than +100 mV, fast inactivation was evident, which indicated that $K_v\beta1.3$ and $K_v1.5$ remained assembled after PKC inhibition and that without PKC activity, the voltage dependence of $K_v\beta1.3$-induced inactivation is dramatically shifted in the positive direction. Additionally, we demonstrate that $K_v1.5$+$K_v\beta1.3$ channels interacted with RACK1, PKCβI, PKCβII, and PKCθ, either directly or through scaffold proteins, generating an emerging $K_v1.5$ channelosome in HEK293 cells and ventricular tissue.

EXPERIMENTAL PROCEDURES

Expression Plasmids, Cell Culture, and Transient Transfection—Human $K_v1.5$ and $K_v\beta1.3$ in pBK have been extensively characterized (4). Human $K_v1.5$ (−22 to 1,894 nucleotides) and $K_v\beta1.3$ (−53 to 1,500 nucleotides) were inserted into the same pBK vector, with the $K_v1.5$ subunit placed 3′ to the $K_v\beta1.3$ subunit and preceded by an internal ribosome entry sequence, thus generating a bicistronic messenger RNA as described previously (9). The gene encoding $K_v\beta1.3$ was subcloned between the SacII and NotI restriction sites within the polylinker of the pCMV-Tag5A vector, which generated a recombinant $K_v\beta1.3$-Myc protein. To generate $K_v2.1$-HA, the HA epitope was inserted after Gly-217 of the rat $K_v2.1$ cDNA, placing the epitope in the extracellular S1-S2 loop (41). In some experiments, a construct with an HA tag introduced into the $K_v1.5$ S1-S2 loop was used (kindly provided by Prof. D. J. Snyders).

HEK293 cells were cultured in Dulbecco's modified Eagle's medium supplemented with 10% fetal bovine serum, 10 units/ml penicillin-streptomycin (Sigma-Aldrich), and 1% nonessential amino acids. For the electrophysiological experiments, cells were transfected with $K_v1.5$ (0.4 μg) or $K_v1.5$+$K_v\beta1.3$ channels (0.3 μg) and a reporter plasmid expressing CD8 (1.6 μg) using Lipofectamine 2000 (10 μl) (Invitrogen). Before experimental use, the cells were incubated with polystyrene microbeads precoated with an anti-CD8 antibody (Dynabeads M450, Dynal) as described previously (5, 7, 42). For the immunocytochemistry and immunoprecipitation studies, the cells were cotransfected with 0.5 μg of $K_v1.5$ or $K_v2.1$-HA and 1 μg of $K_v\beta1.3$-Myc cDNA.

Inhibitors, Antibodies, and siRNA—Calphostin C, Gö6976, Gö6983, hispidin, and PKCζ pseudosubstrate inhibitor (PKCζ-PI) were from Calbiochem (Merck KGaA). Donkey anti-goat antibody was from Santa Cruz Biotechnology (Santa Cruz, CA), and goat anti-mouse and goat anti-rabbit antibodies were from Calbiochem (1:10000); all of them were horseradish peroxidase-conjugated. The polyclonal rabbit antibody anti-$K_v1.5$ (1:1000) was purchased from Alomone Labs, the monoclonal anti-Myc (1:500) and anti-β-actin (1:40000) antibodies were from Santa Cruz Biotechnology, anti-$K_v\beta1$ (1:500) was from Abcam (Abcam Limited), and anti-HA (1:250) was from Novus (Novus Biologicals). Monoclonal antibodies specific for the PKC isoforms (1:200) and anti-RACK1 (1:500) were from Santa Cruz Biotechnology.

To knock down all PKC isoforms, we transfected HEK293 cells with PKC-specific small interfering RNAs (siRNAs) purchased from Santa Cruz Biotechnology, according to the manufacturer's instructions. The PKC siRNA contains five target-specific 19–25-nucleotide siRNAs that are designed to knock down gene expression. The most efficient transfection results were obtained with 50 nM of the siRNA duplexes transfected 72 h prior to the experiments.

Electrophysiological Recordings and Data Acquisition—The intracellular pipette filling solution contained the following (in mM): 80 potassium aspartate, 42 KCl, 3 phosphocreatine, 10 KH_2PO_4, 3 MgATP, 5 HEPES-K, and 5 EGTA-K (adjusted to pH 7.25 with KOH). The bath solution contained the following (in mM): 140 NaCl, 4 KCl, 1.8 $CaCl_2$, 1 $MgCl_2$, 10 HEPES-Na, and 10 glucose (adjusted to pH 7.40 with NaOH). Currents were recorded using the whole-cell configuration of the patch clamp technique with a patch clamp amplifier (Axopatch-200B patch clamp amplifier; Molecular Devices) and stored on a personal computer (TD Systems) with a DigiData 1440A analog-to-digital converter (Molecular Devices). PClamp version 10 software was used for both data acquisition and analysis (Molecular Devices). Currents were recorded at room temperature (21–23 °C) at a stimulation frequency of 0.1 Hz and were sampled at 4 kHz after antialias filtering at 2 kHz. The average pipette resistance ranged between 1 and 3 megaohms ($n = 70$). Gigaohm seal formation was achieved by suction (2–5 gigaohms, $n = 70$). After seal formation, the cells were lifted from the bath, and the membrane patch was ruptured with a brief additional suction. The capacitive transients elicited by symmetrical 10-mV steps from −80 mV were recorded at 50 kHz and filtered at 10 kHz for subsequent calculations of the capacitive surface area, access resistance, and input impedance. Thereafter, the capacitance and series resistance compensation were optimized, and usually 80% compensation of the effective access resistance was obtained. MicroCal Origin 7.05 (OriginLab Co) and the Clampfit utility of pClamp 9 were used to perform least squares fitting and for data presentation. Deactivation and inactivation were fitted to a biexponential process with an equation of the form $y = A_1\exp(-t/\tau_1) + A_2\exp(-t/\tau_2) + C$, where τ_1 and τ_2 are the system time constants, A_1 and A_2 are the amplitudes of each component of the exponential, and C is the baseline value. The voltage dependence of the activation curves was fitted with a Boltzmann equation: $y = 1/(1 + \exp(-(V - V_h)/s))$, where s represents the slope factor, V represents the membrane potential, and V_h represents the voltage at which 50% of the channels are open.

Protein Extracts, Immunoprecipitation, and Western Blot—For total protein extraction from HEK293 cells, the cells were washed twice in chilled phosphate-buffered saline (PBS) and centrifuged at 3,000 × *g* for 10 min. The pellet was then lysed in ice-cold lysis solution (20 mM HEPES, pH 7.4, 1 mM EDTA, 255 mM sucrose supplemented with Complete protease inhibitor mixture tablets (Roche Diagnostics)), and homogenized by repeated passage (10 times) through a 25-gauge (0.45 × 16 mm) needle. Homogenates were further centrifuged at 10,000 × *g* for 5 min to remove nuclei and organelles. Samples were separated into aliquots and stored at −80 °C. For immunoprecipitation assays, we isolated membrane protein from the total protein extract by an additional centrifugation at ~150,000 × *g* for 90 min. The pellet was resuspended in 30 mM HEPES (pH 7.4), and the protein content was determined using the Bradford Bio-Rad protein assay (Bio-Rad). Ventricular (principal coronary arteries excluded) and atrial tissues from male Wistar rats were kindly provided by Drs. A. Cogolludo and F. Pérez-Vizcaíno (Universidad Complutense de Madrid, Spain). After dissection, cardiac tissue was frozen in liquid nitrogen and homogenized in a glass potter (300 μl and 3 ml of the lysis buffer described above were used for atria and ventricles, respectively). The homogenate was centrifuged at 6000 × *g* for 10 min at 4 °C. The supernatant was collected, separated into aliquots, and stored at −80 °C until its posterior analysis.

For the coimmunoprecipitation experiments, the homogenates were resuspended in 150 μl of immunoprecipitation buffer (1% Nonidet P-40, 10% glycerol, 10 mM HEPES, and 150 mM NaCl supplemented with Complete protease inhibitor mixture tablets (pH = 7.8) (Roche Diagnostics)) and homogenized by orbital shaking at 4 °C for 1 h. 300 μg of crude membrane protein was used for HEK293 cells, 500 μg was used for rat atria, and 1500 μg was used for the ventricular tissue. Proteins were then incubated with 20 μl of immunoprecipitation buffer-prewashed Sepharose protein A/G beads (Santa Cruz Biotechnology) for 2 h at 4 °C, and contaminant-bound Sepharose beads were separated by centrifugation for 30 s at 5000 × *g* at 4 °C. The supernatant was incubated with 4 ng of polyclonal anti-$K_v1.5$ (Alomone Labs) or monoclonal anti-RACK1 antibody (Santa Cruz Biotechnology) for each microgram of protein, overnight at 4 °C with orbital shaking. Approximately 20–30 μl of PBS-washed Sepharose protein A/G beads was then added to the mixture followed by incubation for 2 h. Sepharose beads bound to antibody-protein complexes were precipitated by centrifugation (30 s at 5000 × *g* at 4 °C), and antibody-bound beads were then washed twice with immunoprecipitation buffer and centrifuged for 30 s at 5000 × *g* at room temperature. In the case of cardiac tissue samples, coimmunoprecipitation was performed using Pierce® Direct IP kit (Thermo Scientific) following the manufacturer's instructions.

Total protein extracts and immunoprecipitated protein samples were resuspended in 1× SDS (2% β-mercaptoethanol) and boiled at 100 °C for 5 min. The samples were then centrifuged for 3 min at 5,000 × *g* at room temperature, and 25–50 μl of protein extract was separated by SDS-PAGE (7, 10, or 15% acrylamide/bisacrylamide) gels. The proteins, transferred to PVDF membranes, were probed with anti-$K_v1.5$, anti-Myc, anti-PKC, anti-$K_v\beta1$, and anti-RACK1 antibodies. Secondary antibodies were developed by ECL-Plus Western blotting reagent (Amersham Biosciences).

Immunostaining and Confocal Microscopy—For immunostaining, HEK293 cells were grown on gelatin-coated coverslips in Dulbecco's modified Eagle's medium containing 10% fetal bovine serum. Twenty-four hours after transfection, the cells were washed three times with PBS. For antibody-induced patching experiments, after 30 min of incubation with blocking solution (10% goat serum, 5% nonfat dry milk, PBS), the cells were incubated with the S1-S2 $K_v1.5$ external epitope antibody (diluted 1:1000) or anti-HA (diluted 1:250) in HEPES-based culture medium for 1 h at room temperature (43). Next, the cells were fixed with 4% paraformaldehyde in PBS for 10 min and blocked overnight (PBS + 5% w/v dry milk). The cells were washed and permeabilized three times with PBS-CHAPS and then incubated with anti-Myc antibody (1:500; PBS-CHAPS with 10% goat serum). Next, the cells were washed three times with PBS-CHAPS and incubated with Alexa Fluor 488 anti-rabbit (1:500) and Alexa Fluor 594 anti-mouse (1:500) antibodies from Molecular Probes. The samples were mounted with

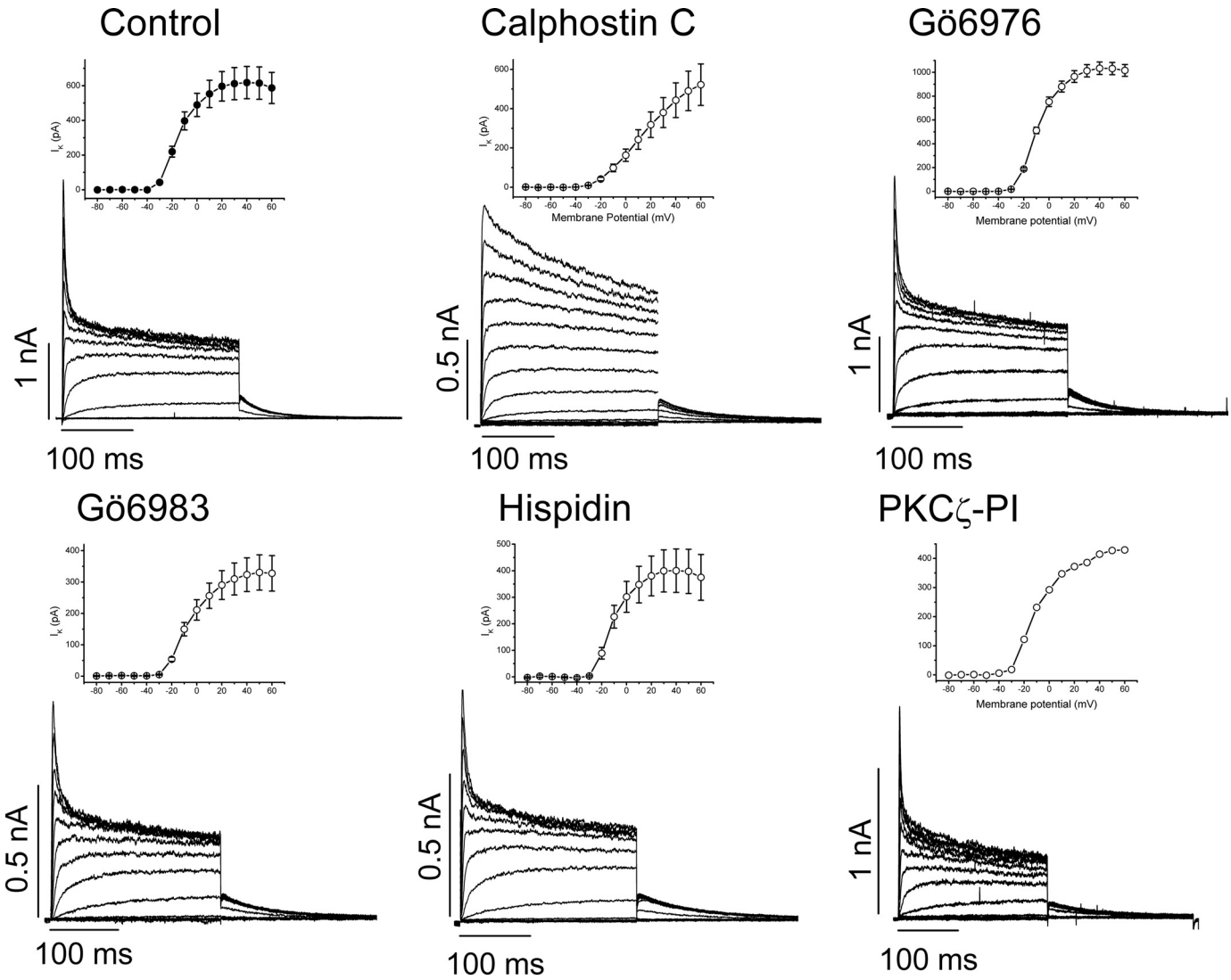

FIGURE 1. **Modulation of $K_v\beta1.3$-induced fast inactivation is not due to a single PKC isoform.** HEK293 cells were transiently transfected with $K_v1.5+K_v\beta1.3$. Representative current traces elicited by 250-ms depolarizing pulses from a holding potential of −80 mV to voltages between −80 and +60 mV in 10-mV steps and the *IV* relationships in which the current magnitude measured at the end of 250-ms pulses was plotted *versus* the membrane potential are shown. Tail currents were obtained upon return to −40 mV. The specific inhibitor used is indicated above each trace family.

Aqua Poly/Mount (Polysciences, Inc). Stained cells were visualized using LSM510 ZEISS (Carl Zeiss) or Leica TCS SP5 confocal microscopes, and images were analyzed with Zeiss, Leica, and ImageJ software (44).

Statistical Analysis—Data are presented as the mean ± S.E. One-way analysis of variance was used to compare more than two groups. Statistical significance was set at $p < 0.05$. The curve-fitting procedure used a nonlinear least squares (Gauss-Newton) algorithm; the results are displayed in a linear and semilogarithmic format together with the difference plot. Goodness of fit was determined using the χ^2-square criterion and by inspection of systematic nonrandom trends in the difference plot.

RESULTS

Modulation of $K_v\beta1.3$-induced Fast Inactivation Is Not Driven by a single PKC Isoform—Although PKC inhibition prevents $K_v\beta1.3$-induced fast inactivation of $K_v1.5$ channels (9–11), the identity of the specific isoform responsible for this phenomenon remains unknown. To that end, we first determined which PKC isoforms are expressed in HEK293 cells. Supplemental Fig. S1 shows that HEK293 cells express all PKC isoforms (classical: α, β, and γ; novel: δ, ϵ, and θ; and atypical: ζ and λ/ι) with the exception of the novel PKCη isoform.

Next, we performed electrophysiological experiments using different PKC inhibitors. Fig. 1 shows representative current traces obtained under control conditions and after PKC inhibition with different inhibitors. The characteristics of these PKC inhibitors are shown in Table 1. With the exception of calphostin C, PKC inhibitors (Gö6976, Gö6983, hispidin, and PKCζ-PI) failed to abolish $K_v\beta1.3$-induced fast inactivation. Only after PKC inhibition with calphostin C did the current-voltage relationship (*IV*) exhibit the linearity observed when the $K_v1.5$ current is recorded in the absence of $K_v\beta1.3$. Different mechanisms of action of PKC inhibitors may explain these results. Table 2 shows the values obtained for the degrees of inactiva-

tion, V_h, and the inactivation and deactivation kinetics (τ) of the currents generated after treating the cells with various PKC inhibitors. Remarkably, all of the tested PKC inhibitors decreased the degree of fast inactivation and slowed the fast time constant of the inactivation process (Table 2).

TABLE 1

Primary and secondary targets of the different PKC inhibitors used in the present study

MLCK, myosin light-chain kinase.

Inhibitor	IC_{50}	Primary target	Secondary target
Calphostin C	50 nM	Classical and novel PKC isoforms	MLCK, PKA, PKG, p60v-src
Gö6976	2 nM, 6 nM	PKCα, PKCβI	PKD (IC_{50} = 20 nM)
Gö6983	7 nM	Classical and novel PKC isoforms	PKCζ (IC_{50} = 60 nM)
Hispidin	2 μM	PKCβ	

TABLE 2

Electrophysiological characteristics of the $K_v1.5+K_v\beta1.3$ current following exposure to different PKC inhibitors

Data represent the mean ± S.E. τ_{fast}: fast inactivation kinetics; τ_{slow}: slow inactivation kinetics; τ_{deac}: deactivation kinetics; V_h: half-voltage of activation. Statistically significant differences are indicated by asterisks.

	Concentration	Inactivation	τ_{fast}	τ_{slow}	τ_{deac}	V_h
	μM	%	ms	ms	ms	mV
Control	0	70 ± 2	3.5 ± 0.3	120 ± 8.2	47 ± 0.4	−21 ± 0.7
Calphostin C	0.2, 3	32 ± 6*	103 ± 32[a]		108 ± 24*	−8 ± 3*
Gö6976	0.2	57 ± 0.2*	10 ± 0.7*	124 ± 8.5	51 ± 6	−20 ± 3.4
Gö6983	5	60 ± 3*	6 ± 0.9*	152 ± 22	63 ± 3*	−17 ± 0.7*
Hispidin	5	59 ± 2*	5 ± 0.5*	104 ± 9*	58 ± 0.4*	−19 ± 0.6

[a] The inactivation process of $K_v1.5+K_v\beta1.3$ channels after treatment with calphostin C could only be fitted to a monoexponential equation.

siRNA-induced Down-regulation of PKC Mimics Effects of Calphostin C—The results presented above could be explained by either (*a*) an effect that requires inhibition of different PKC isoforms or (*b*) a direct effect of calphostin C that is independent of its PKC inhibitory properties. To differentiate between these two possibilities, we performed a series of experiments in which all PKC isoforms were silenced using siRNA (PKC siRNA). The greatest PKC silencing was observed 72 h after transient transfection of siRNA duplexes at a concentration of 50 nM (Fig. 2*A*). In the present study, PKC siRNA led to an ~75% decrease in expression of the various PKC isoforms (Fig.

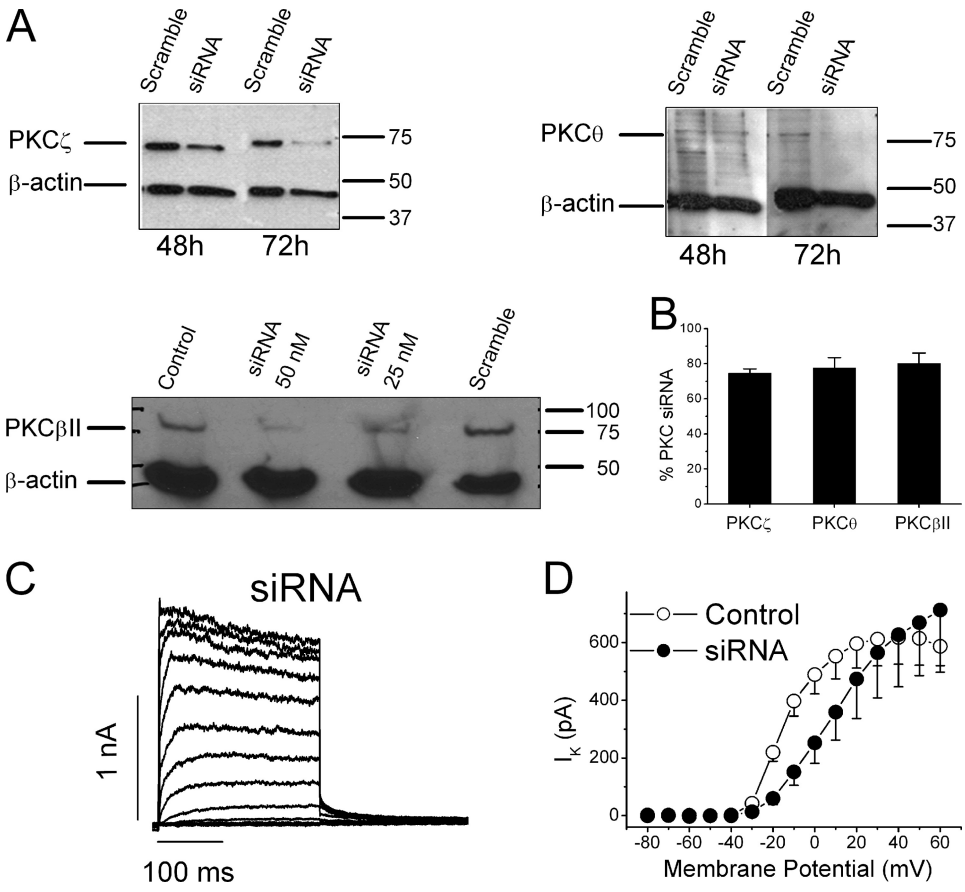

FIGURE 2. **Abolishment of fast inactivation by PKC siRNA.** *A*, Western blots to detect PKCζ and PKCθ, two of the PKCs present in HEK293 cells transfected with either scrambled or 50 nM siRNA duplexes after 48 and 72 h of transfection (*top panel*). Note that the highest efficiency was obtained, in both cases, after 72 h of transfection. *Bottom panel*: PKCβII expression in controls (untransfected cells) after transfection with 50 and 25 nM PKC siRNA and scrambled siRNA. Immunodetection was performed 72 h after transfection. *B*, graph showing the percentage of PKC siRNA obtained in HEK293 cells measured by Western blot. The values were quantified to those of β-actin (n = 3). *C*, effects of PKC siRNA on the $K_v1.5+K_v\beta1.3$ current. *D*, *IV* relationships obtained by plotting the current magnitude measured at the end of 250-ms depolarizing pulses *versus* the membrane potential. Patch clamp experiments were repeated at least six times, and Western blotting was performed at least three times. Reproducible results were obtained using both experimental techniques.

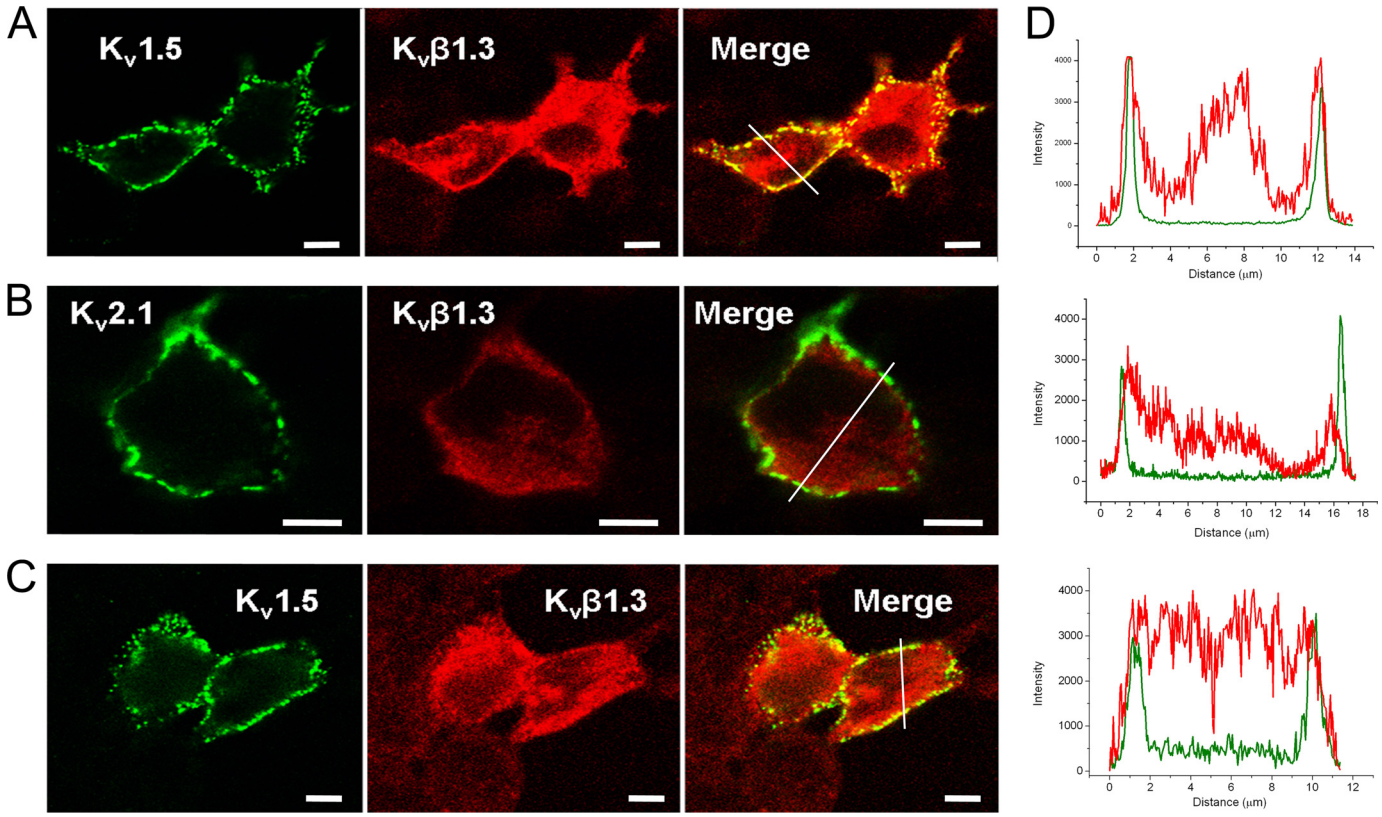

FIGURE 3. **Immunocytochemical staining of $K_v1.5$ and $K_v\beta1.3$-Myc subunits using antibody-induced patching.** *A*, positive control. Colocalization of the subunits appears as *yellow membrane clusters* due to the merge of the green ($K_v1.5$) and red ($K_v\beta1.3$-Myc) channels after detection with secondary fluorescent antibodies. *B*, negative control. $K_v2.1$-HA and $K_v\beta1.3$-Myc channels do not assemble. Thus, they were used as a negative control for colocalization. Lack of colocalization is visualized as an absence of yellow fluorescence. *C*, calphostin C-treated (200 nM) cells transiently transfected with $K_v1.5$+$K_v\beta1.3$-Myc; *yellow fluorescence* is evident in patches of the membrane, indicating colocalization of $K_v1.5$ and $K_v\beta1.3$-Myc subunits in the cell membrane. In all pictures, the *bar* represents 5 μm. *D*, histograms of the pixel-by-pixel analysis of the section indicated by *lines* in *Merge panels* in *A*, *B*, and *C*, respectively.

2*B*, supplemental Table S1). Fig. 2*C* shows non-inactivating electrophysiological recordings of the $K_v1.5$+$K_v\beta1.3$ channels after PKC siRNA treatment. Voltage-dependent potassium currents were evoked by applying depolarizing pulses from a holding potential of −80 mV to different voltages between −80 to +60 mV in 10-mV steps. Fig. 2*D* shows the *IV* relationships measured at the end of the 250-ms pulses under these experimental conditions. Under control conditions, the *IV* relationship reached a plateau at around +15 mV. Binding of the inactivating particle of the $K_v\beta1.3$ subunit is a highly voltage-dependent process; at more positive test potentials, this binding is more likely to occur. PKC siRNA eliminated fast inactivation, and thus, the *IV* relationships obtained under these experimental conditions resembled those obtained after activation of $K_v1.5$ channels in the absence of $K_v\beta1.3$ subunits (7). Hence, this treatment mimicked the effects of calphostin C on the current generated after activation of $K_v1.5$+$K_v\beta1.3$ channels, which ruled out a possible direct effect of calphostin C.

$K_v1.5$ and $K_v\beta1.3$ Still Colocalize in Cell Membrane during PKC Inhibition—If the inhibition of PKC affects the assembly of these subunits, a physical dissociation of both proteins in the cell membrane should be detected. To further test the above hypothesis, we used two different experimental approaches. First, we performed a series of experiments in which the $K_v1.5$ and $K_v\beta1.3$-Myc subunits were stained using antibody-induced patching. This method of immunostaining is based on the formation of antibody-induced membrane patches after labeling an external epitope of the $K_v1.5$ channel located in the S1-S2 loop (using a custom-made polyclonal antibody that recognizes this epitope). Fig. 3*A* shows the colocalization of $K_v1.5$ and $K_v\beta1.3$-Myc (n = 28). This pattern is specific because, as expected, $K_v2.1$ and $K_v\beta1.3$-Myc (n = 8), which do not coassemble (45, 46), did not colocalize (Fig. 3*B*). Interestingly, we did not detect differences in the degree of colocalization between control and calphostin C-treated cells (n = 29) (Fig. 3*D*).

Given the widespread cellular distribution of $K_v\beta1.3$, we next analyzed via immunoprecipitation whether $K_v1.5$ and $K_v\beta1.3$ remained associated with $K_v1.5$ following calphostin C-mediated PKC inhibition. Fig. 4*A* shows that $K_v1.5$ protein was immunoprecipitated in the presence but not in the absence of anti-$K_v1.5$ antibody. As shown in Fig. 4*B*, we did not observe any $K_v\beta1.3$-Myc signal in untransfected cells or in cells transfected with $K_v1.5$ alone. However, the $K_v\beta1.3$ subunit remained associated with $K_v1.5$ under control conditions and after calphostin C treatment, which suggests that these proteins do not dissociate following treatment with calphostin C.

Positive Potentials Up to +100 mV Reveal Presence of $K_v\beta1.3$—Assembly of the $K_v\beta1.3$ subunit causes fast inactivation of the $K_v1.5$ outward current (45, 47–49). Therefore, it was surprising to observe that even when these subunits remained assembled, $K_v\beta1.3$-induced fast inactivation was abolished either by inhibition of PKC with calphostin C or by silencing PKC.

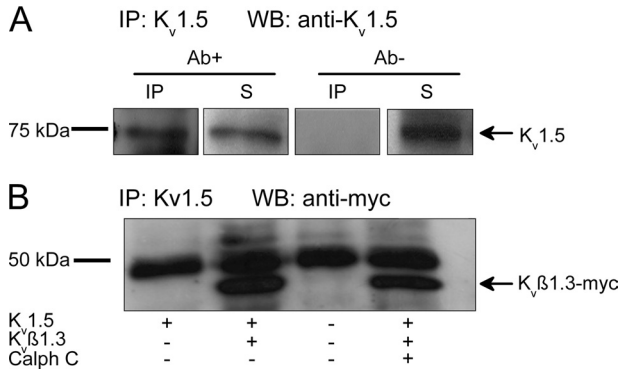

FIGURE 4. **Immunoprecipitation of $K_v1.5$ with $K_v\beta1.3$-Myc.** *A*, negative (*Ab*−) and positive (*Ab*+) control immunoprecipitations (*IP*) blotted against $K_v1.5$ channels. Supernatants (*S*) are also shown. *WB*, Western blot. *B*, immunoprecipitation of $K_v1.5$ channels and blotting against $K_v\beta1.3$-Myc revealed the coimmunoprecipitation of both subunits, indicating that the protein assembly was not abolished by PKC inhibition. The *arrow* indicates the Kvβ1.3-Myc epitope. The band that appears with a molecular mass of 50 kDa corresponds to the immunoglobulin heavy chain.

$K_v1.5$+$K_v\beta1.3$ current is activated at −30 mV and inactivates at potentials positive to 0 mV, exhibiting a degree of inactivation of 70 ± 2% (n = 23) when measured at +60 mV (Fig. 1). After PKC inhibition with calphostin C- or siRNA-mediated PKC silencing, $K_v1.5$+$K_v\beta1.3$ currents showed a degree of slow inactivation that ranged between 20 and 30%, whereas pulse steps to potentials positive to +60 mV revealed the presence of the typical $K_v\beta1.3$-induced fast inactivation (Fig. 5*A*). Fig. 5*A* also shows the mean values of the inactivation degrees obtained at +100 mV recorded in at least four experiments. These results further suggest that $K_v1.5$ and $K_v\beta1.3$ remain assembled after PKC inhibition.

This outcome suggests that after PKC inhibition, the inactivation curve of $K_v1.5$-$K_v\beta1.3$ current is shifted toward more positive membrane potentials. To test this hypothesis, a series of experiments was performed in which a double-pulse protocol was applied (Fig. 5*B*). These results show that the inactivation curve in calphostin C-treated cells was shifted toward more positive potentials (V_h = −26.5 ± 0.6 *versus* −8.5 ± 1.9 mV in the presence and in the absence of calphostin C, respectively; n = 10; see Fig. 5*C* and Table 3). Moreover, the degree of inactivation in calphostin C-treated cells decreased from 47.3 ± 5.7% (n = 5) to 34.6 ± 2.2% (n = 7) ($p < 0.05$).

Effects of PIP_2 and OAG on $K_v\beta1.3$-induced Fast Inactivation—It has been proposed that PIP_2 associates with the N terminus of the $K_v\beta1.3$ subunit, and when the β subunit dissociates from PIP_2, it assumes a hairpin structure that can enter the central cavity of an open $K_v1.5$ channel, triggering N-type inactivation. Therefore, it has been suggested that $K_v\beta1.3$-induced fast inactivation is mediated by equilibrium binding of the N terminus of $K_v\beta1.3$, which switches between binding to phosphoinositides (PIPs) and the inner pore region of $K_v1.5$ channels (50). Moreover, stimulation of α1-receptors activates PLCγ, which is capable of cleaving PIP_2 into IP_3 and DAG, thus activating classical and novel PKCs. Thus, the effects of PIP_2 and OAG (a nondegradable DAG analog) were analyzed by adding them to the internal solution (Fig. 6). Cells dialyzed with PIP_2 exhibited a lower degree of fast inactivation just after patch rupture in comparison with control cells (55 ± 4% *versus* 68 ± 6%, n = 4, $p < 0.05$) (Fig. 6*A*). Also, after 8 min of dialysis with PIP_2, the degree of N-type inactivation increased significantly (from 55 ± 4% to 70 ± 4%, n = 4, $p < 0.05$) (Fig. 6*A*). These effects could be due to a decrease of the PIP_2 concentration due to its cleavage into IP_3 and DAG. In fact, the degradation of PIP_2 would increase the ability of the N terminus of $K_v\beta1.3$ to inactivate $K_v1.5$ (50). In contrast, cells dialyzed with OAG exhibited a degree of N-type inactivation similar to control cells, both after patch rupture and after 8 min of dialysis with OAG (65 ± 3% to 67 ± 2%, n = 5, $p > 0.05$) (Fig. 6*B*). These results are in agreement with the involvement of classical and novel PKC isoforms in the effects of calphostin C and PKC siRNA on the fast $K_v\beta1.3$-induced inactivation. To test whether the PIP_2 effects at different times (t = 0 or 8 min) were due to the cleavage of PIP_2 into DAG and IP_3, a series of experiments in which cells previously incubated with a PLC inhibitor (U73122, 10 μM) and dialyzed with PIP_2 was performed (Fig. 6*C*). Under these experimental conditions, the degree of fast inactivation was reduced (from 69 ± 2% to 62 ± 2%, n = 9, $p < 0.01$), the time constant of the fast inactivation was increased, and the contribution of the fast component of inactivation was decreased.

The $K_v1.5$ Macromolecular Complex Contains $K_v1.5$, $K_v\beta1.3$, RACK1, PKCβI, PKCβII, and PKCθ—Several ion channels have been reported to be modulated by PKC via RACK1 (34). We hypothesized that $K_v1.5$, $K_v\beta1.3$, and PKC form a functional complex in which PKC activity is an essential requirement for the induction of fast and incomplete channel inactivation by $K_v\beta1.3$. To test this hypothesis, immunocytochemistry experiments were performed (Fig. 7). Fig. 7*A* shows confocal images of cells transfected with $K_v1.5$-HA and $K_v\beta1.3$, in which we stained for $K_v1.5$ and RACK1. Fig. 7*B* shows confocal images of cells transfected with $K_v1.5$ and $K_v\beta1.3$-Myc, in which we stained for $K_v\beta1.3$ and RACK1. As shown, under both experimental conditions, colocalization was consistent between $K_v1.5$ and RACK1, as well as between $K_v\beta1.3$ and RACK1. Given the widespread immunolocalization patterns, we confirmed subunit association using immunoprecipitation experiments. We immunoprecipitated $K_v1.5$ channels and blotted for PKCβII to confirm the presence of this enzyme in the protein complexes. As shown in Fig. 8*A*, PKCβII signal was absent in PKC siRNA-transfected cells. Furthermore, blots against RACK1 confirmed the interaction of $K_v1.5$ with this adaptor protein (Fig. 8*B*). Moreover, reverse coimmunoprecipitation (immunoprecipitation of RACK1) yielded similar results, revealing the presence not only of PKCβII (data not shown) but also of the $K_v1.5$ and $K_v\beta1.3$ subunits (Fig. 8*C*). Collectively, these results demonstrate the presence of a functional complex or channelosome that includes $K_v1.5$, $K_v\beta1.3$, RACK1, and PKCβII. This interaction was demonstrated in controls and was found to be absent in PKC-silenced cells (Fig. 8*A*). On the other hand, because calphostin C inhibits PKC by binding to the DAG binding site, the reduced level of PKCβII in calphostin C-treated cells is not surprising, as inhibited PKCβII may not be able to bind RACK1 in the channelosome.

To determine which PKC isoforms are present in this macromolecular complex, a series of coimmunoprecipitation experiments were performed in which we immunoprecipitated $K_v1.5$ channels and blotted for the PKC isoforms

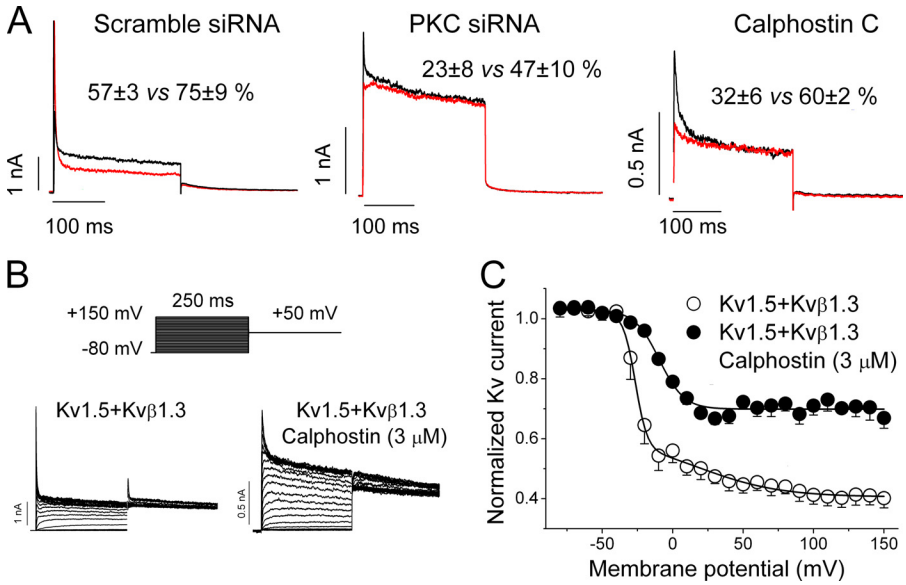

FIGURE 5. **Voltage dependence of inactivation of $K_v1.5$ and $K_v1.5+K_v\beta1.3$.** *A*, current traces obtained after depolarization from a holding potential of −80 mV to +60 (*red*) and +100 mV (*black*) in HEK293 cells transfected with $K_v1.5+K_v\beta1.3$ and with scrambled siRNA (50 nM) (*left*), with PKC siRNA-transfected cells (*middle*) and in calphostin C-treated cells (*right*). *B*, original current records obtained in control and calphostin C-treated cells. *C*, voltage dependence of the inactivation under control and after calphostin C treatment. Note that calphostin C shifts the inactivation curve to more positive potentials.

TABLE 3

Voltage-dependent inactivation parameters

V_h: half voltage of inactivation. *s*: slope of the Boltzmann equation. Data represent the mean ± S.E. of $n = 7$ experiments. Statistically significant differences are indicated by asterisks.

	V_{h1}	V_{h2}	s_1	s_2
	mV	*mV*	*mV*	*mV*
$K_v1.5+K_v\beta1.3$	−26.5 ± 0.6	19.0 ± 0.6	4.2 ± 0.6	28.7 ± 7.8
$K_v1.5+K_v\beta1.3$ (calphostin C μM)	−8.5 ± 1.9*		9.8±.9*	

present in HEK293 cells (Fig. 9). We observed that only PKCβI, PKCβII, and PKCθ were present in the $K_v1.5$ channelosome.

The $K_v1.5$ Channelosome Is Present in Rat Ventricular Myocytes but Not in Atrial Myocytes—Finally, we performed experiments in cardiac tissue (Fig. 10). Coimmunoprecipitation experiments were performed in which we immunoprecipitated $K_v1.5$ channels and blotted for PKCβI, PKCβII, PKCθ, RACK1, and $K_v\beta1.x$. Samples from ventricular homogenates presented a $K_v1.5$ channelosome composed of $K_v1.5$, $K_v\beta1$, RACK1, PKCβI, and PKCβII (Fig. 10*A*). Importantly, atrial tissue did not display this $K_v1.5$ protein complex (Fig. 10*B*) because none of the proteins studied forming the $K_v1.5$ channelosome in ventricle coimmunoprecipitated with $K_v1.5$ in atrial tissue.

DISCUSSION

In the present study, we have analyzed the mechanisms by which calphostin C-mediated PKC inhibition abolishes $K_v\beta1.3$-induced fast inactivation of the $K_v1.5$ channel. We have demonstrated that the inhibition of at least classical and novel PKC isoforms is required to abolish $K_v\beta1.3$-induced fast inactivation (9, 10). Furthermore, this effect was not due to $K_v1.5+K_v\beta1.3$ dissociation but due to a positive shift of the inactivation curve driven by PKC inhibition because both subunits remained assembled as shown by immunocytochemistry, immunoprecipitation, and electrophysiological experiments. We have also shown that at least $K_v\beta1.3$, RACK1, PKCβI, PKCβII, and PKCθ are associated with $K_v1.5$ in HEK293 cells, forming a channelosome. Finally, for the first time, we provide evidence pointing to the existence of a native ventricular cardiac $K_v1.5$ channelosome, whose composition is similar to that found in HEK293 cells (with the exception of PKCθ, absent in this tissue according to our Western blot analyses, data not shown).

The stimulation of α1-receptors leads to activation of PLCγ. This enzyme cleaves PIP_2, generating IP_3 and DAG, which activate most PKC isoforms either alone or with Ca^{2+}, with the exception of atypical PKCs. The N terminus of the $K_v\beta1.3$ subunit associates with membrane-bound PIP_2, and when it dissociates from PIP_2, it assumes a hairpin structure that enters the central cavity of an open $K_v1.5$ channel, inducing fast inactivation. Thus, $K_v\beta1.3$-induced fast inactivation is mediated by a competitive binding between PIPs and the inner pore region of $K_v1.5$ channels for the N terminus of $K_v\beta1.3$ (50). The present results obtained for PIP_2 and OAG are in agreement with previous studies and indicate a fine-tuned regulation of $K_v\beta1.3$-induced fast inactivation by PKC and PIP_2. Moreover, the effects of PIP_2 in cells in which the PLC was inhibited produced a marked decrease of the $K_v\beta1.3$-induced fast inactivation. In the absence of PIP_2 into the internal solution, the effects observed were qualitatively similar (data not shown), suggesting a role of PLC on the fast inactivation induced by this β subunit.

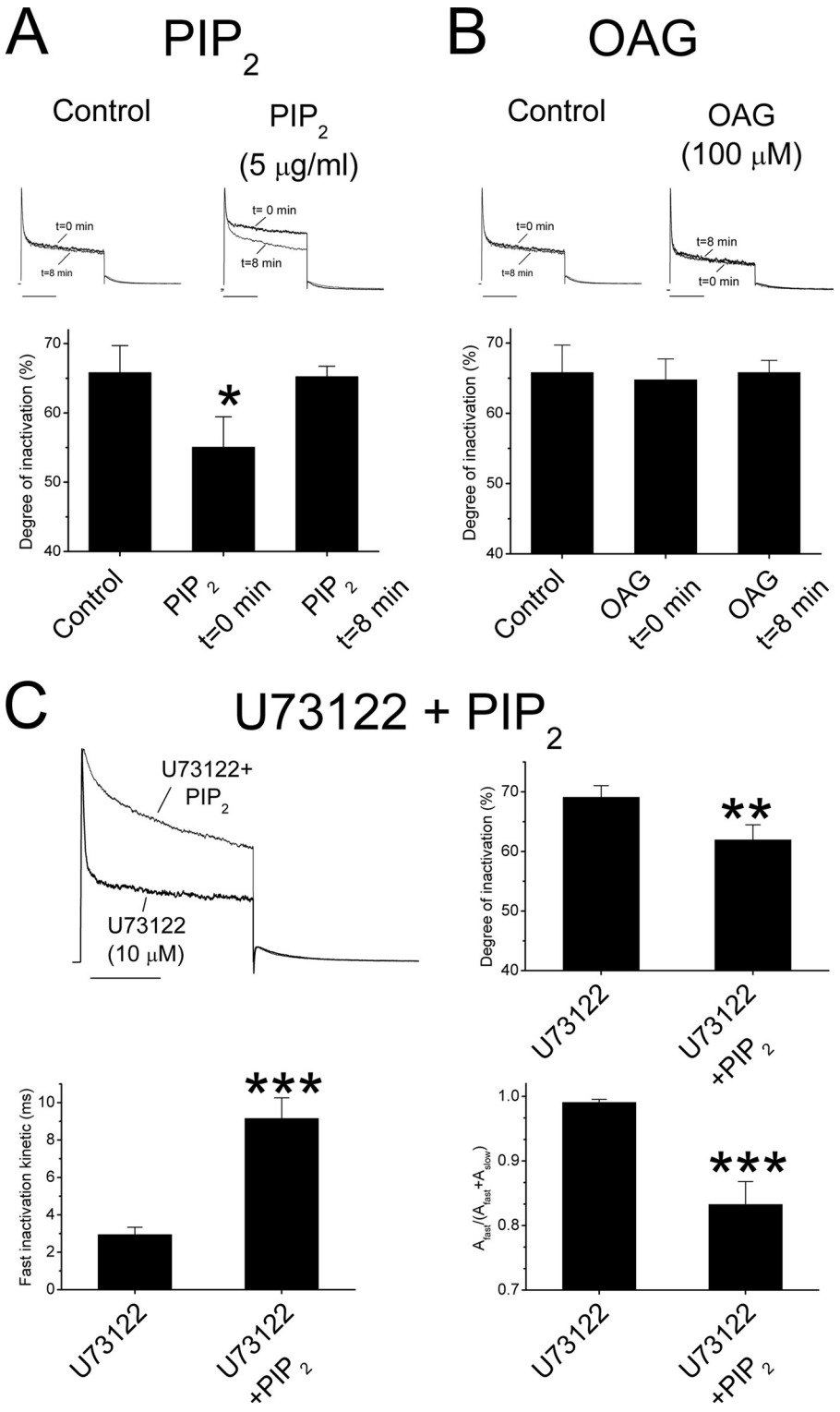

FIGURE 6. **Effects of PIP_2, OAG, and PLC on $K_v\beta1.3$-induced fast inactivation.** *A*, representative current traces obtained after depolarization from a holding potential of −80 mV to +60 mV, just after patch rupture ($t = 0$ min) and after 8 min ($t = 8$ min), in control conditions and during PIP_2 dialysis. The graph shows the degree of inactivation in control cells and in cells dialyzed with PIP_2 at $t = 0$ min and $t = 8$ min. Note that at $t = 0$, the degree of fast inactivation was significantly lower than that after 8 min of dialysis in PIP_2 and control dialyzed cells. *B*, representative current traces obtained at +60 mV at $t = 0$ and $t = 8$ min in control conditions and during OAG dialysis. The graph shows the degree of fast inactivation in control cells and in cells dialyzed with OAG at $t = 0$ min and $t = 8$ min. The degree of fast inactivation was similar in all experimental conditions. *C*, representative current traces obtained at +60 mV at $t = 0$ (U73122, 10 μM) and $t = 8$ min (U73122 + PIP_2) after inhibition of PLC with U73122 and after PIP_2 dialysis. The *upper right*, *bottom left*, and *bottom right* graphs show the degree of fast inactivation, the fast inactivation kinetics, and the contribution of the fast component of inactivation to the total process ($A_{fast}/(A_{fast} + A_{slow})$) under both experimental conditions, respectively. *, $p < 0.05$; **, $p < 0.01$; ***, $p < 0.001$.

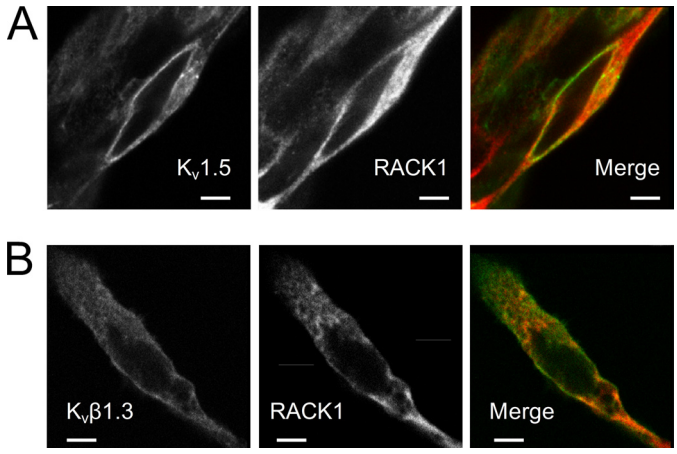

FIGURE 7. **Immunocytochemical staining of $K_v1.5$-HA or $K_v\beta1.3$-Myc and RACK1 proteins.** *A*, cells stained with anti-$K_v1.5$-HA, anti-$K_v\beta1.3$-Myc, or anti-RACK1. Colocalization appears as *yellow fluorescence* due to the merge of the green ($K_v1.5$-HA) and red (RACK1) channels after detection with secondary fluorescent antibodies. Cells were cotransfected with $K_v1.5$-HA + $K_v\beta1.3$-Myc. RACK1 is an endogenous protein. *B*, cells stained with anti-Myc (*green*) and anti-RACK1 (*red*). Cells were transfected with $K_v\beta1.3$-Myc alone. In all pictures, the *bar* represents 5 μm.

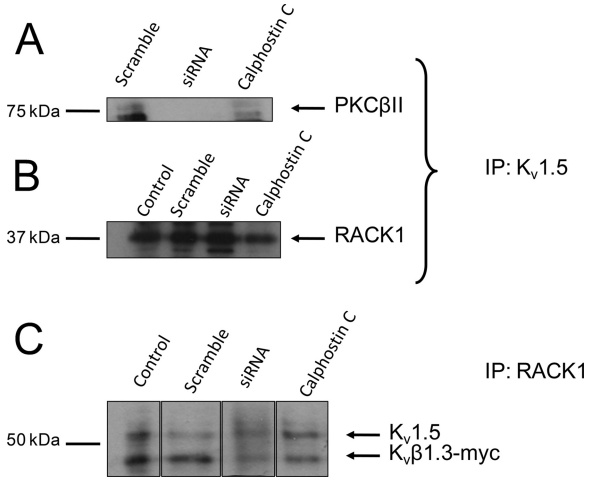

FIGURE 8. **Immunoprecipitation of $K_v1.5+K_v\beta1.3$ channel or RACK1 with PKCβII.** *A*, PKCβII coimmunoprecipitated (*IP*) with $K_v1.5$. *B*, RACK1 coimmunoprecipitated with $K_v1.5$ under all experimental conditions. The results are representative of three independent experiments. *C*, coimmunoprecipitation of RACK1 and immunodetection of $K_v1.5$ and c-Myc-tagged $K_v\beta1$.

Most PKC isoforms redistribute into different subcellular compartments upon activation, depending on the PKC isoform and the cell type (36). A surprising finding of the present study was that all of the PKC inhibitors tested (Gö6976, Gö6983, hispidin, and PKCζ-PI), with the exception of calphostin C, failed to abolish $K_v\beta1.3$-induced fast inactivation. This result is likely due to the different mechanisms of action of the PKC inhibitors used. Indeed, calphostin C inhibits PKC by binding to its C1 domain (DAG and phorbol ester binding site) and then irreversibly inactivates the enzyme. Gö6983 and Gö6976 are competitive inhibitors of ATP binding to the catalytic domain of PKC, whereas hispidin affects both PKCβI and PKCβII translocation (23, 51–54). Our results suggest that inhibition of classical and novel, but not atypical, PKC isoforms counteracts $K_v\beta1.3$-induced fast inactivation and shifts the V_h of the activation curve to values closer to those of $K_v1.5$ observed in the absence of $K_v\beta1.3$, as has been described previously (9). The potential dissociation of α-β caused by PKC inhibition was also analyzed in the present study. Colocalization, immunoprecipitation, and electrophysiological experiments revealed that these subunits remained assembled in the plasma membrane despite PKC inhibition by calphostin C. These results are in agreement with the notion that $K_v1.5$ and $K_v\beta1.3$ subunits assemble in the endoplasmic reticulum during the early stages of their biosynthesis (55), and a 2-h incubation with calphostin C is sufficient to eliminate the typical fast inactivation induced by $K_v\beta1.3$ (9). Moreover, previous results reported by Kwak *et al.* (9) showed that a tandem construction of $K_v1.5$ and $K_v\beta1.3$, which generates a unique protein, showed similar responses to calphostin C (a shift in V_h to more positive potentials and a loss of fast inactivation). These results indicate that mechanisms other than subunit dissociation must be involved in the abolishment of $K_v\beta1.3$-induced fast inactivation produced by calphostin C.

Although we were able to rule out a role for atypical PKCs, the involvement of a specific PKC isoform in this process has not yet been demonstrated. In addition, experiments in which the membrane potential was depolarized to +100 mV indicated that despite PKC inhibition (calphostin C or PKC siRNA), $K_v\beta1.3$ was still capable of conferring fast inactivation and thus remained associated with $K_v1.5$. Furthermore, the coimmunoprecipitation experiments showed that $K_v\beta1.3$ remained associated with $K_v1.5$ despite PKC inhibition by calphostin C or by PKC silencing by siRNA. These data suggest that $K_v1.5$ and $K_v\beta1.3$ subunits form a stable complex following their biosynthesis in the endoplasmic reticulum and that PKC inhibition and/or activation modulates the inactivating effect of $K_v\beta1.3$. It has been demonstrated that residues Arg-5 and Thr-6 of the $K_v\beta1.3$ subunit are involved in PIP_2 binding and that mutations (alanine or cysteine) at these residues dramatically increase the degree of $K_v\beta1.3$-induced fast inactivation. It has been described that calphostin C does not modify the gating of the $K_v1.5$ in the absence of β subunits (9). Therefore, it is likely that the effects shown in the present study involve the phosphorylation of some residues present in the $K_v\beta1.3$ subunit. One candidate could be threonine at position 6 (Thr-6) of $K_v\beta1.3$. Thus, we may hypothesize that PKC phosphorylation of this threonine or another threonine/serine at the N terminus of the $K_v\beta1.3$ subunit can lead to a diminished capability to bind PIP_2, thus avoiding the abrogation of fast inactivation caused by PIP_2. These findings provide an explanation for the effects of PKC inhibition on the $K_v\beta1.3$-induced inactivation, assuming that phosphorylated $K_v\beta1.3$ cannot bind PIP_2. Nonphosphorylated $K_v\beta1.3$ would be able to bind PIP_2, and this binding would abolish N-type inactivation (50). However, further experiments are necessary to elucidate the residue(s) involved in this effect.

In the past decade, myriads of protein-protein interactions involved in intracellular signaling have been described (56–59). Determination of the subcellular localization of signal transduction proteins, enzymes, substrates, and mediators has revealed the rapid, efficient transmission of signals either from the extracellular medium or from intracellular sites as an essential feature of optimal signaling (60). Despite the high degree of homology between PKC isoforms at both sequence and struc-

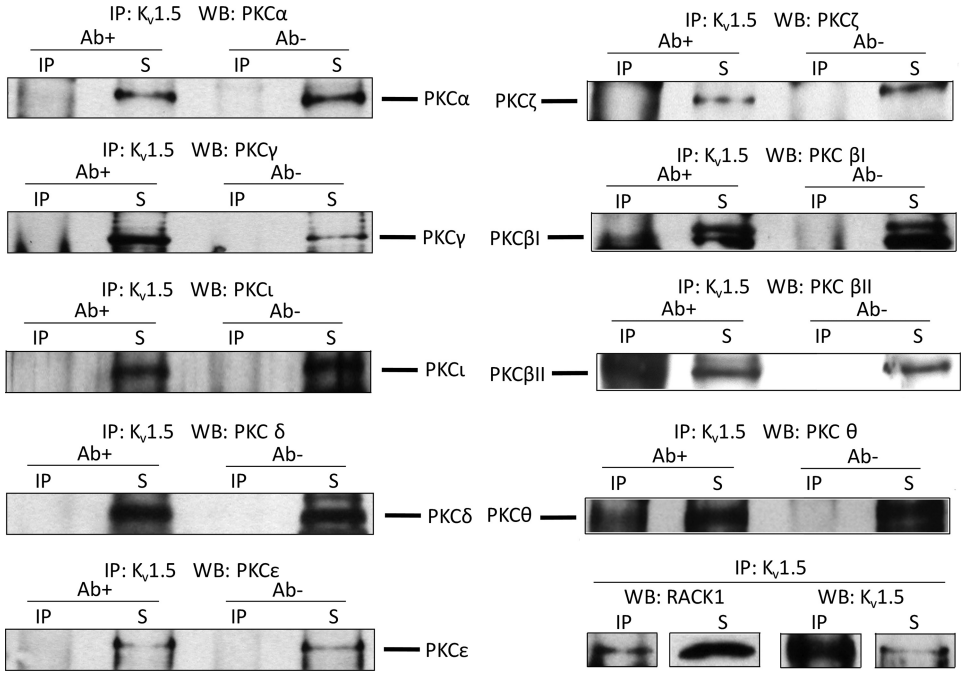

FIGURE 9. **Immunoprecipitation of K_v1.5+$K_v\beta$1.3 channel with PKCs ($n = 3$).** Negative (*Ab*−) and positive (*Ab*+) immunoprecipitations (*IP*) blotted against the different PKCs isoforms present in HEK293 cells. Note that only PKCβI, PKCβII, and PKCθ coimmunoprecipitated with K_v1.5+$K_v\beta$1.3 channels. *WB*, Western blot; *S*, supernatants.

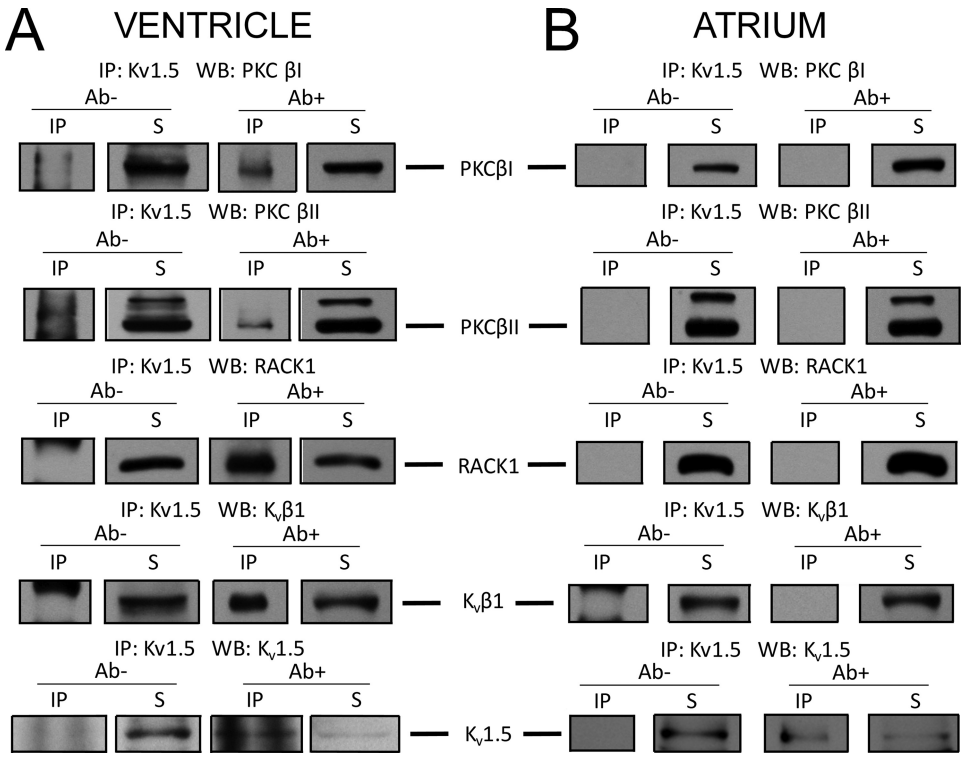

FIGURE 10. **Immunoprecipitation of K_v1.5 channel in cardiac tissue ($n = 3$).** Negative (*Ab*−) and positive (*Ab*+) immunoprecipitations (*IP*) blotted against the different PKC isoforms present in HEK293 channelosome (Fig. 9). Note that a very similar channelosome has been found in ventricular (*A*), but not in atrial (*B*), tissue. *WB*, Western blot; *S*, supernatants.

tural levels, especially within the catalytic domain, each PKC isoform mediates unique subcellular functions (29, 30) that are dependent on the target substrate (26, 31). These localization mechanisms are especially common in plasma membrane proteins because incoming stimuli must be integrated and transmitted with a high degree of efficiency. In the present study, we have demonstrated that K_v1.5 and $K_v\beta$1.3 form a highly stable protein complex, which is tightly regulated by classical and novel, but not atypical, PKC isoforms. Furthermore, our results show that PKCβI, PKCβII, and RACK1 coassemble with K_v1.5 and $K_v\beta$1.3. Therefore, the K_v1.5 functional channelosome contains at least K_v1.5, $K_v\beta$1.3, RACK1, PKCβI, PKCβII, and

PKCθ. Besides, a similar channelosome has been found in ventricular tissue, but not in atrial tissue, showing a parallel distribution to that of $K_v\beta1.3$ (47), which suggests an important role of this β subunit in the constitution of the macromolecular complex.

The presence of RACK1 in other ion channel complexes has been previously reported. Indeed, RACK1 binds to the carboxyl terminus of $K_{Ca}1.1$ channels (35). Moreover, the overexpression of RACK1 with $K_{Ca}1.1$ channels in *Xenopus* oocytes shifts the activation curve toward more positive potentials in the absence, but not in the presence, of ectopically expressed β channel subunits (35). Furthermore, PKCβII, which is recruited by RACK1, down-regulates $Ca_v1.2$ activity following activation (36). Besides, the functional $K_{ir}3.1$ complex contains PKA, protein phosphatase 1 (PP1), PP2A/C, and RACK1. Within this complex, RACK1 binds directly to G$\beta\gamma$ (37) and PKC (34). Recently, it has been described that TRPC3 regulates IP_3 receptor (IP_3R) function by mediating interaction between IP_3R and the scaffolding protein RACK1, and the importance of the Orai1-STIM1-TRPC3-RACK1-IP_3R complexes in the fine modulation of intracellular Ca^{2+} stimulated by agonists of these receptors has been reported (38). Thus, RACK1 is emerging as an important adaptor protein that may play very important roles in the modulation of different ion channels and in the interaction between ion pores and ancillary subunits. The variety of signaling proteins linked to RACK1 (32), which include PKCβII (34, 40), PLCγ (61), *Src* (62), and dynamin-1 (63), among others, could explain the diverse effects of PKA and PKC on the $K_v1.5+K_v\beta1.3$ current (8–11) and the requirement for simultaneous inhibition of numerous PKC isoforms to abolish fast inactivation.

In conclusion, we have analyzed the mechanisms by which calphostin C abolishes $K_v\beta1.3$-induced fast inactivation. Our experiments demonstrate that this effect is not due to the dissociation of $K_v1.5$ and $K_v\beta1.3$ subunits and that these subunits remain assembled following PKC inhibition. Our experiments additionally demonstrate that PLC is also involved in the regulation of the Kvβ1.3-induced fast inactivation.

In addition, we have characterized a $K_v1.5$ channelosome in which $K_v1.5$, $K_v\beta1.3$, RACK1, PKCβI, PKCβII, and PKCθ physically and functionally interact. Importantly, we have identified a very similar macromolecular complex in rat ventricular tissue. The description and functional characterization of this channelosome open up a variety of possible mechanisms to explain the differences between I_{Kur} recorded in ventricle and atrium in different animal species. Differential composition of this $K_v1.5$ complex could constitute a primary mechanism of capital importance for the modulation of cardiac excitability.

Acknowledgments—We thank U. Lyakhovych for technical assistance and Drs. L. Sastre, A. Cogolludo, and F. Perez-Vizcaíno for valuable comments and discussions regarding this manuscript. We thank the editorial assistance of American Journal Experts.

REFERENCES

1. Fedida, D., Wible, B., Wang, Z., Fermini, B., Faust, F., Nattel, S., and Brown, A. M. (1993) Identity of a novel delayed rectifier current from human heart with a cloned K^+ channel current. *Circ. Res.* **73,** 210–216
2. Snyders, D. J., Tamkun, M. M., and Bennett, P. B. (1993) A rapidly activating and slowly inactivating potassium channel cloned from human heart: Functional analysis after stable mammalian cell culture expression. *J. Gen. Physiol.* **101,** 513–543
3. Uebele, V. N., England, S. K., Chaudhary, A., Tamkun, M. M., and Snyders, D. J. (1996) Functional differences in $K_v1.5$ currents expressed in mammalian cell lines are due to the presence of endogenous $K_v\beta2.1$ subunits. *J. Biol. Chem.* **271,** 2406–2412
4. Uebele, V. N., England, S. K., Gallagher, D. J., Snyders, D. J., Bennett, P. B., and Tamkun, M. M. (1998) Distinct domains of the voltage-gated K^+ channel $K_v\beta1.3$ β subunit affect voltage-dependent gating. *Am. J. Physiol.* **274,** C1485–C1495
5. González, T., Navarro-Polanco, R., Arias, C., Caballero, R., Moreno, I., Delpón, E., Tamargo, J., Tamkun, M. M., and Valenzuela, C. (2002) Assembly with the $K_v\beta1.3$ subunit modulates drug block of $hK_v1.5$ channels. *Mol. Pharmacol.* **62,** 1456–1463
6. Decher, N., Kumar, P., Gonzalez, T., Renigunta, V., and Sanguinetti, M. C. (2005) Structural basis for competition between drug binding and $K_v\beta1.3$ accessory subunit-induced N-type inactivation of $K_v1.5$ channels. *Mol. Pharmacol.* **68,** 995–1005
7. Arias, C., Guizy, M., David, M., Marzian, S., González, T., Decher, N., and Valenzuela, C. (2007) $K_v\beta1.3$ reduces the degree of stereoselective bupivacaine block of $K_v1.5$ channels. *Anesthesiology* **107,** 641–651
8. Li, G. R., Feng, J., Wang, Z., Fermini, B., and Nattel, S. (1996) Adrenergic modulation of ultrarapid delayed rectifier K^+ current in human atrial myocytes. *Circ. Res.* **78,** 903–915
9. Kwak, Y. G., Navarro-Polanco, R. A., Grobaski, T., Gallagher, D. J., and Tamkun, M. M. (1999) Phosphorylation is required for alteration of $K_v1.5$ K^+ channel function by the $K_v\beta1.3$ subunit. *J. Biol. Chem.* **274,** 25355–25361
10. Kwak, Y. G., Hu, N., Wei, J., George, A. L., Jr., Grobaski, T. D., Tamkun, M. M., and Murray, K. T. (1999) Protein kinase A phosphorylation alters $K_v\beta1.3$ subunit-mediated inactivation of the $K_v1.5$ potassium channel. *J. Biol. Chem.* **274,** 13928–13932
11. Murray, K. T., Fahrig, S. A., Deal, K. K., Po, S. S., Hu, N. N., Snyders, D. J., Tamkun, M. M., and Bennett, P. B. (1994) Modulation of an inactivating human cardiac K^+ channel by protein kinase C. *Circ. Res.* **75,** 999–1005
12. Schlaich, M. P., Kaye, D. M., Lambert, E., Sommerville, M., Socratous, F., and Esler, M. D. (2003) Relation between cardiac sympathetic activity and hypertensive left ventricular hypertrophy. *Circulation* **108,** 560–565
13. Schlaich, M. P., Kaye, D. M., Lambert, E., Hastings, J., Campbell, D. J., Lambert, G., and Esler, M. D. (2005) Angiotensin II and norepinephrine release: interaction and effects on the heart. *J. Hypertens.* **23,** 1077–1082
14. Takeishi, Y., Jalili, T., Ball, N. A., and Walsh, R. A. (1999) Responses of cardiac protein kinase C isoforms to distinct pathological stimuli are differentially regulated. *Circ. Res.* **85,** 264–271
15. Kerkelä, R., Ilves, M., Pikkarainen, S., Tokola, H., Ronkainen, J., Vuolteenaho, O., Leppäluoto, J., and Ruskoaho, H. (2002) Identification of PKCα isoform-specific effects in cardiac myocytes using antisense phosphorothioate oligonucleotides. *Mol. Pharmacol.* **62,** 1482–1491
16. Braz, J. C., Bueno, O. F., De Windt, L. J., and Molkentin, J. D. (2002) PKCα regulates the hypertrophic growth of cardiomyocytes through extracellular signal-regulated kinase1/2 (ERK1/2). *J. Cell Biol.* **156,** 905–919
17. Hahn, H. S., Marreez, Y., Odley, A., Sterbling, A., Yussman, M. G., Hilty, K. C., Bodi, I., Liggett, S. B., Schwartz, A., and Dorn, G. W. (2003) Protein kinase Cα negatively regulates systolic and diastolic function in pathological hypertrophy. *Circ. Res.* **93,** 1111–1119
18. Tessier, S., Karczewski, P., Krause, E. G., Pansard, Y., Acar, C., Lang-Lazdunski, M., Mercadier, J. J., and Hatem, S. N. (1999) Regulation of the transient outward K^+ current by Ca^{2+}/calmodulin-dependent protein kinases II in human atrial myocytes. *Circ. Res.* **85,** 810–819
19. Kühlkamp, V., Schirdewan, A., Stangl, K., Homberg, M., Ploch, M., and Beck, O. A. (2000) Use of metoprolol CR/XL to maintain sinus rhythm after conversion from persistent atrial fibrillation: a randomized, double-blind, placebo-controlled study. *J. Am. Coll. Cardiol.* **36,** 139–146
20. Workman, A. J., Kane, K. A., Russell, J. A., Norrie, J., and Rankin, A. C. (2003) Chronic β-adrenoceptor blockade and human atrial cell electrophysiology: evidence of pharmacological remodeling. *Cardiovasc. Res.* **58,**

518–525
21. Valenzuela, C. (2003) Pharmacological electrical remodeling in human atria induced by chronic β-blockade. *Cardiovasc. Res.* **58,** 498–500
22. Williams, C. P., Hu, N., Shen, W., Mashburn, A. B., and Murray, K. T. (2002) Modulation of the human $K_v1.5$ channel by protein kinase C activation: role of the $K_v\beta1.2$ subunit. *J Pharmacol. Exp. Ther.* **302,** 545–550
23. Kobayashi, E., Nakano, H., Morimoto, M., and Tamaoki, T. (1989) Calphostin C (UCN-1028C), a novel microbial compound, is a highly potent and specific inhibitor of protein kinase C. *Biochem. Biophys. Res. Commun.* **159,** 548–553
24. Mellor, H., and Parker, P. J. (1998) The extended protein kinase C superfamily. *Biochem. J.* **332,** 281–292
25. Nishizuka, Y. (1988) The molecular heterogeneity of protein kinase C and its implications for cellular regulation. *Nature* **334,** 661–665
26. Carpenter, D., Jackson, T., and Hanley, M. R. (1987) Protein kinase Cs: coping with a growing family. *Nature* **325,** 107–108
27. Dai, S., Hall, D. D., and Hell, J. W. (2009) Supramolecular assemblies and localized regulation of voltage-gated ion channels. *Physiol. Rev.* **89,** 411–452
28. Souroujon, M. C., and Mochly-Rosen, D. (1998) Peptide modulators of protein-protein interactions in intracellular signaling. *Nat. Biotechnol.* **16,** 919–924
29. Dempsey, E. C., Newton, A. C., Mochly-Rosen, D., Fields, A. P., Reyland, M. E., Insel, P. A., and Messing, R. O. (2000) Protein kinase C isozymes and the regulation of diverse cell responses. *Am. J. Physiol. Lung Cell. Mol. Physiol.* **279,** L429–L438
30. Jaken, S., and Parker, P. J. (2000) Protein kinase C binding partners. *Bioessays* **22,** 245–254
31. Parker, P. J., Kour, G., Marais, R. M., Mitchell, F., Pears, C., Schaap, D., Stabel, S., and Webster, C. (1989) Protein kinase C: a family affair. *Mol. Cell. Endocrinol.* **65,** 1–11
32. Schechtman, D., and Mochly-Rosen, D. (2001) Adaptor proteins in protein kinase C-mediated signal transduction. *Oncogene* **20,** 6339–6347
33. Neer, E. J., Schmidt, C. J., Nambudripad, R., and Smith, T. F. (1994) The ancient regulatory-protein family of WD repeat proteins. *Nature* **371,** 297–300
34. Ron, D., Chen, C. H., Caldwell, J., Jamieson, L., Orr, E., and Mochly-Rosen, D. (1994) Cloning of an intracellular receptor for protein kinase C: a homolog of the β subunit of G proteins. *Proc. Natl. Acad. Sci. U.S.A.* **91,** 839–843
35. Isacson, C. K., Lu, Q., Karas, R. H., and Cox, D. H. (2007) RACK1 is a BKCa channel-binding protein. *Am. J. Physiol. Cell Physiol.* **292,** C1459–C1466
36. Dorn, G. W., 2nd, and Mochly-Rosen, D. (2002) Intracellular transport mechanisms of signal transducers. *Annu. Rev. Physiol.* **64,** 407–429
37. Dell, E. J., Connor, J., Chen, S., Stebbins, E. G., Skiba, N. P., Mochly-Rosen, D., and Hamm, H. E. (2002) The βγ subunit of heterotrimeric G proteins interacts with RACK1 and two other WD repeat proteins. *J. Biol. Chem.* **277,** 49888–49895
38. Woodard, G. E., López, J. J., Jardín, I., Salido, G. M., and Rosado, J. A. (2010) TRPC3 regulates agonist-stimulated Ca^{2+} mobilization by mediating the interaction between type I inositol 1,4,5-trisphosphate receptor, RACK1, and Orai1. *J. Biol. Chem.* **285,** 8045–8053
39. Yaka, R., Thornton, C., Vagts, A. J., Phamluong, K., Bonci, A., and Ron, D. (2002) NMDA receptor function is regulated by the inhibitory scaffolding protein, RACK1. *Proc. Natl. Acad. Sci. U.S.A.* **99,** 5710–5715
40. Csukai, M., Chen, C. H., De Matteis, M. A., and Mochly-Rosen, D. (1997) The coatomer protein β′-COP, a selective binding protein (RACK) for protein kinase Cε. *J. Biol. Chem.* **272,** 29200–29206
41. O'Connell, K. M., and Tamkun, M. M. (2005) Targeting of voltage-gated potassium channel isoforms to distinct cell surface microdomains. *J. Cell Sci.* **118,** 2155–2166
42. González, T., Longobardo, M., Caballero, R., Delpón, E., Tamargo, J., and Valenzuela, C. (2001) Effects of bupivacaine and a novel local anesthetic, IQB-9302, on human cardiac K^+ channels. *J. Pharmacol. Exp. Ther.* **296,** 573–583
43. Mays, D. J., Foose, J. M., Philipson, L. H., and Tamkun, M. M. (1995) Localization of the $K_v1.5$ K^+ channel protein in explanted cardiac tissue. *J. Clin. Invest.* **96,** 282–292
44. Bréchet, A., Fache, M. P., Brachet, A., Ferracci, G., Baude, A., Irondelle, M., Pereira, S., Leterrier, C., and Dargent, B. (2008) Protein kinase CK2 contributes to the organization of sodium channels in axonal membranes by regulating their interactions with ankyrin G. *J. Cell Biol.* **183,** 1101–1114
45. England, S. K., Uebele, V. N., Shear, H., Kodali, J., Bennett, P. B., and Tamkun, M. M. (1995) Characterization of a voltage-gated K^+ channel β subunit expressed in human heart. *Proc. Natl. Acad. Sci. U.S.A.* **92,** 6309–6313
46. Rhodes, K. J., Keilbaugh, S. A., Barrezueta, N. X., Lopez, K. L., and Trimmer, J. S. (1995) Association and colocalization of K^+ channel α and β subunit polypeptides in rat brain. *J. Neurosci.* **15,** 5360–5371
47. England, S. K., Uebele, V. N., Kodali, J., Bennett, P. B., and Tamkun, M. M. (1995) A novel K^+ channel β subunit ($hK_v\beta1.3$) is produced via alternative mRNA splicing. *J. Biol. Chem.* **270,** 28531–28534
48. Leicher, T., Roeper, J., Weber, K., Wang, X., and Pongs, O. (1996) Structural and functional characterization of human potassium channel subunit β1 (KCNA1B). *Neuropharmacology* **35,** 787–795
49. Hoshi, T., Zagotta, W. N., and Aldrich, R. W. (1990) Biophysical and molecular mechanisms of Shaker potassium channel inactivation. *Science* **250,** 533–538
50. Decher, N., Gonzalez, T., Streit, A. K., Sachse, F. B., Renigunta, V., Soom, M., Heinemann, S. H., Daut, J., and Sanguinetti, M. C. (2008) Structural determinants of $K_v\beta1.3$-induced channel inactivation: a hairpin modulated by PIP2. *EMBO J.* **27,** 3164–3174
51. Qatsha, K. A., Rudolph, C., Marmé, D., Schächtele, C., and May, W. S. (1993) Gö6976, a selective inhibitor of protein kinase C, is a potent antagonist of human immunodeficiency virus 1 induction from latent/low-level-producing reservoir cells in vitro. *Proc. Natl. Acad. Sci. U.S.A.* **90,** 4674–4678
52. Young, L. H., Balin, B. J., and Weis, M. T. (2005) Gö6983: a fast acting protein kinase C inhibitor that attenuates myocardial ischemia/reperfusion injury. *Cardiovasc. Drug Rev.* **23,** 255–272
53. Wadsworth, S. J., and Goldfine, H. (2002) Mobilization of protein kinase C in macrophages induced by *Listeria monocytogenes* affects its internalization and escape from the phagosome. *Infect. Immun.* **70,** 4650–4660
54. Sossin, W. S. (1997) An autonomous kinase generated during long-term facilitation in Aplysia is related to the Ca^{2+}-independent protein kinase C Apl II. *Learn Mem.* **3,** 389–401
55. Nagaya, N., and Papazian, D. M. (1997) Potassium channel α and β subunits assemble in the endoplasmic reticulum. *J. Biol. Chem.* **272,** 3022–3027
56. Burack, W. R., and Shaw, A. S. (2000) Signal transduction: hanging on a scaffold. *Curr. Opin. Cell Biol.* **12,** 211–216
57. Hubbard, M. J., and Cohen, P. (1993) On target with a new mechanism for the regulation of protein phosphorylation. *Trends Biochem. Sci.* **18,** 172–177
58. Wang, H., Zhang, Y., Cao, L., Han, H., Wang, J., Yang, B., Nattel, S., and Wang, Z. (2002) HERG K^+ channel, a regulator of tumor cell apoptosis and proliferation. *Cancer Res.* **62,** 4843–4848
59. Mochly-Rosen, D. (1995) Localization of protein kinases by anchoring proteins: a theme in signal transduction. *Science* **268,** 247–251
60. Pawson, T., and Nash, P. (2003) Assembly of cell regulatory systems through protein interaction domains. *Science* **300,** 445–452
61. Disatnik, M. H., Hernandez-Sotomayor, S. M., Jones, G., Carpenter, G., and Mochly-Rosen, D. (1994) Phospholipase C-γ1 binding to intracellular receptors for activated protein kinase C. *Proc. Natl. Acad. Sci. U.S.A.* **91,** 559–563
62. Chang, B. Y., Conroy, K. B., Machleder, E. M., and Cartwright, C. A. (1998) RACK1, a receptor for activated C kinase and a homolog of the β subunit of G proteins, inhibits activity of Src tyrosine kinases and growth of NIH 3T3 cells. *Mol. Cell. Biol.* **18,** 3245–3256
63. Rodriguez, M. M., Ron, D., Touhara, K., Chen, C. H., and Mochly-Rosen, D. (1999) RACK1, a protein kinase C anchoring protein, coordinates the binding of activated protein kinase C and select pleckstrin homology domains *in vitro*. *Biochemistry* **38,** 13787–13794